

## CONDITION MONITORING OF A ROTATING MACHINE USING HOLOSPECTRUM

**André Garcia Chiarello**

Departamento de Mecânica, Universidade Federal de Itajubá, CP.50, CEP 37500-903, Itajubá, Brasil,  
e-mail: andregc@unifei.edu.br.

**Abstract** Traditional methods for practical condition monitoring of rotating machinery are usually based on spectral analysis and shaft orbit diagrams. These conventional methods are very effective for monitoring operational parameters and also for fault diagnosis. However, different machine faults may present the same spectral representation and also they may produce virtually negligible alteration in orbit diagrams. To improve the efficiency of the conventional methods for condition monitoring, this paper proposes the application of the holo spectrum method using a high resolution spectrum. The holo spectrum is based on ellipses, which are constructed using both, frequency and phase information of radial shaft vibrations. The frequencies of interest, which are used in the holo spectrum, must be precisely calculated and to achieve this purpose, a high resolution spectrum method is proposed. The high resolution spectrum calculates the main frequencies of the signal with a desired frequency resolution and showed satisfactory results with simulated signals. These characteristics are important because the ellipses calculated in the holo spectrum are not perturbed by noise and contain only relevant system informations. The holo spectrum method has been applied in a vertical test machine for condition monitoring. The results showed that small variations in some operational parameters, which are not well detected by orbit diagrams and spectral analysis, are easily detected by the holo spectrum method. The diagrams visualized in the holo spectrum are geometrically simple and these characteristics facilitate the task of associating each diagram to the respective machine condition.

**Keywords:** Holo spectrum, condition monitoring, spectral resolution, orbit diagrams.

### 1. Introduction

The conventional methods for condition monitoring of practical rotating machinery are usually based on spectral analysis and shaft orbit diagrams. The Fast Fourier Transform (FFT) of vibration signals is the basic mathematical tool for calculating the spectral representation, which is usually analyzed in the form of amplitude and phase diagrams. The spectral analysis is an efficient method for detecting faults that are clearly related with the synchronous frequency of the rotor, for example: the shaft unbalance produces an increase in the amplitude of the synchronous frequency. In the case of rotating machinery, the vibration signals measured from any part of the machine can be used for spectral analysis; however, the rotor vibrations are one of the most important sources of information about the dynamic behavior of the system. It is well known that a mechanical fault produces alteration in the spectral representation and one can try to associate each fault to its respective spectral representation. Unfortunately, real rotating machinery usually presents complex dynamic behavior and hence, its spectral representation is also complicated. The frequencies related to the rotating components (gears, couplings, bearings) are usually selected as frequencies of interest for condition monitoring purposes. The visualization of any modification of amplitude and phase information of these selected frequencies are interpreted as a symptom of a machine fault.

Another conventional method for practical machinery condition monitoring is the analysis of the shaft orbit diagrams, which represent the trajectory of the center of the shaft in an orthogonal x-y plane. It is expected that any rotor malfunction leads to a modification in the shape of shaft vibration and also to a modification in the orbit diagrams. For a health machine, the orbit diagram is ideally equal to a small circle, considering that a small rotor unbalance is always present. A shaft bow, a misalignment coupling and many others rotor faults usually produce representative shaft orbit diagrams, which can be identified by inspection and comparison with orbit diagrams of a healthy machine. Because of these characteristics, the identification of shaft orbit plays an important role for fault diagnosis of rotating machinery.

The frequencies of interest for monitoring rotating machinery are usually defined equal to the rotor angular velocity (its harmonics and sub-harmonics are also important) but, any other frequency, which is previously identified as a frequency associated to a specific fault, can be also selected. The most common malfunction in rotating machinery is the rotor unbalance. The centrifugal force, which rotates at a synchronous frequency, transfers the rotational energy to transverse shaft vibration and as a result, almost a circular orbit diagram is produced. The second common fault in rotating machinery is the coupling misalignment between two rotors. The axial load produced by rotor misalignment change twice in each shaft revolution and consequently, the harmonic component equal to twice the synchronous frequency, becomes strong in the FFT spectrum. More complex dynamic behavior is produced in the presence of rubbing between rotor and stator. The rubbing involves several physical effects (friction, impacting and non-linearity) and as a result, a large number of strong harmonic components will appear in the FFT spectrum and the original orbit becomes more irregular and complicated (Shi et al, 2004).

Practical rotating machinery is manufactured and assembled with mechanical and electrical components, which have obviously limited manufacturing tolerance. This fact implies that some level of imperfection is always present and the

practical result is a discrepancy between the theoretical and the practical dynamic behavior. If a rotor unbalance occurs, for example, one can expect an orbit diagram not exactly equal to a perfect circle. Therefore, the use of FFT and orbit diagrams for practical machinery monitoring should not be considered completely reliable for extracting diagnostic features directly. To extract reliable and simple diagnostic features from the orbit diagrams it is necessary to develop methods for orbit purification (Peng et al, 2002). One of the simplest methods of orbit purification is to construct an orbit using only the most important rotor frequencies, where all frequencies not related to rotor faults are eliminated from the signals.

The spectral representation and the orbit diagrams represent a class of diagnostic methods based on machine symptoms and as any other diagnostic method based on machine symptoms; patterns of a healthy machine must be extracted a priori. Hence, it is necessary to determine the spectral representation and the orbit diagrams for the machine without faults. After this, each specific fault of interest must be determined and its respective spectral representation and its representative orbit diagrams are calculated. The fault diagnosis can be achieved by comparing the actual patterns with the healthy and fault patterns.

The fault diagnosis process is usually more complicated than the process of fault detection. The main difficulty in the fault diagnosis, based on machine symptoms, is to construct a clear and unique correlation between the fault type and its respective fault pattern. Once this relation is known, it is possible to create some automated routine for fault diagnosis. Artificial intelligence, neural networks or any other method of pattern recognition can be used for fault diagnosis. Recently, Cempel (2003) described a multidimensional condition monitoring based on singular value decomposition. This author has demonstrated that the extraction of fault-related symptoms, which are usually redundant in nature, can be transformed into independent (non-redundant) fault indices and this seems to be important, as it can create reliability of condition monitoring of systems in operation.

Another problem that arises in using spectral analysis and orbit diagrams is that incipient faults may be interpreted as a regular variation of machine parameters. A small malfunction or an incipient fault, in general, produces negligible spectral and orbit pattern modifications. In a previous work, Chiarello and Schwartz (2003) have used the pseudo-phase portrait method for identifying small modifications of operational parameters in a vertical test machine. In this particular application, the small variations of axial load applied to the thrust bearing are not well identified by both FFT spectra neither by orbit diagrams. These aspects suggest that methods for machine condition, that are sensible to small dynamic modifications, are important for detecting a fault at an initial stage.

In this work, a new method of condition monitoring, named holospectrum, is described and compared with conventional methods for detecting small variations in some operational parameters of a practical rotating machine.

## 2. The holospectrum

The holospectrum method has been recently used for practical machinery fault detection and diagnosis (Qu et al 1989, Qu, 1989, Chen et al 1995), and will be briefly described here. The holospectrum is composed by a number of ellipses, each representing a fundamental frequency of a pair of sensors used for monitoring shaft orbits. Denoting by  $x(k)$  and  $y(k)$ , the sampled values of the radial shaft vibrations in two orthogonal planes and computing the discrete Fourier transform (DFT) of both signals in the form  $X(f_k) = DFT\{x(k)\}$  and  $Y(f_k) = DFT\{y(k)\}$ , one can calculate the major and minor axis of the corresponding ellipse in the holospectrum at frequency  $f_k$  as follows:

$$2a(k) = \sqrt{A(k)+B(k)} + \sqrt{A(k)-B(k)}, \quad 2b(k) = \sqrt{A(k)+B(k)} - \sqrt{A(k)-B(k)} \quad (1)$$

where,

$$A(k) = Re^2(X(f_k)) + Im^2(X(f_k)) + Re^2(Y(f_k)) + Im^2(Y(f_k)) \quad (2)$$

$$B(k) = 2 \left| \sqrt{Re^2(X(f_k)) + Im^2(X(f_k))} \sqrt{Re^2(Y(f_k)) + Im^2(Y(f_k))} \sin(\phi_x(f_k) - \phi_y(f_k)) \right| \quad (3)$$

$$\phi_x(f_k) = \arctan \frac{Im(X(f_k))}{Re(X(f_k))}, \quad \phi_y(f_k) = \arctan \frac{Im(Y(f_k))}{Re(Y(f_k))} \quad (4)$$

From the above equations it can be seen that the ellipse axes are calculated using the amplitude and phase information from  $x(k)$  and  $y(k)$  frequency spectra. The inclination angle between the major axis and the horizontal axis is:

$$c(k) = \cos^{-1} \pm \sqrt{\frac{D}{E}} \quad (5)$$

where,

$$D = 1 - \left[ \frac{b(k)}{\sqrt{\operatorname{Re}^2(X(f_k)) + \operatorname{Im}^2(X(f_k)) \sin(\phi_y(f_k) - \phi_x(f_k))}} \right]^2, E = 1 - \left[ \frac{b(k)}{a(k)} \right]^2 \quad (6)$$

In Eq.(5) a positive sign is used if  $\cos(\phi_y(f_k) - \phi_x(f_k)) > 0$ , otherwise, a negative sign is used. The indices  $a(k)$ ,  $b(k)$  and  $c(k)$  describe the shape of the ellipse, which in turn describes the signal spatial correlation (Chen et al, 1995). If both, major and minor ellipses axis are equal, the ellipse becomes a circle, but the phase between the signals is  $90^\circ$  apart.

The holospectrum method has been calculated for simple sinusoidal signals with different characteristics. The Fig. (1A) illustrates a numerical simulation of two sinusoidal signals, which have the same amplitude and the same fundamental frequency, but the phase between the signals is  $90^\circ$ . Condition 1 shows a circle because both sinusoids have the same amplitude, however, in condition 2 the amplitude of sinusoid in direction  $x$  is twice bigger than the amplitude of sinusoid in direction  $y$ . As a result, the major axis of the respective ellipse is twice bigger than the minor axis. The condition 1 of Fig.(1B) shows the holospectrum for two signals where the amplitude in direction  $y$  is twice bigger than the amplitude in direction  $x$  but the angle between the major axis and the  $x$  direction has been changed to  $90^\circ$ . The condition 2 of Fig.(1B) shows an ellipse with a different inclination angle because the phase between the signals is different from  $90^\circ$ .

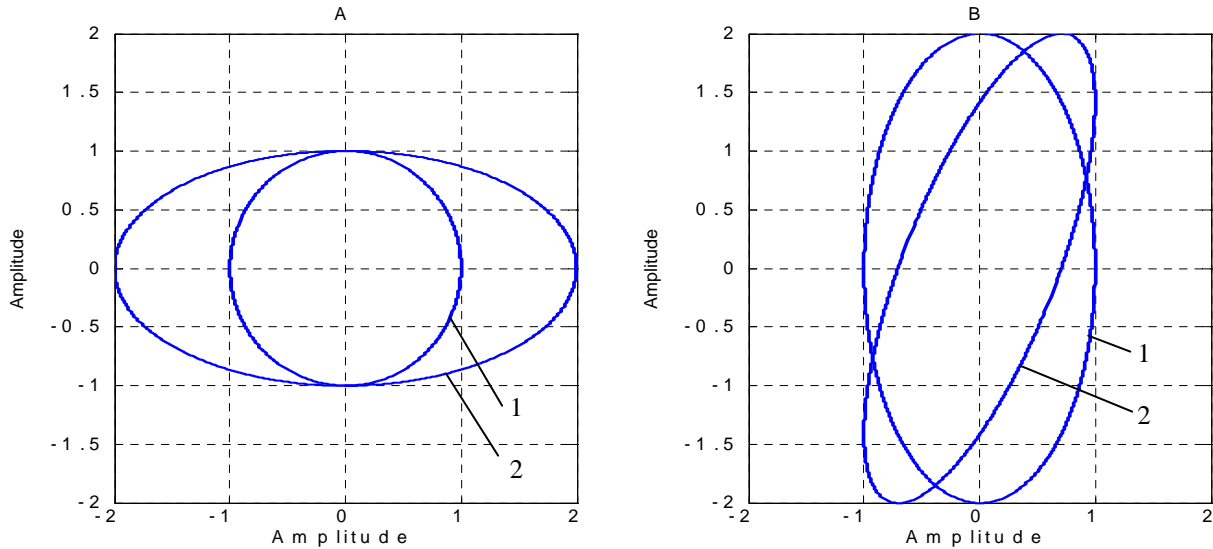


Figure 1. Holospectrum of simple sinusoidal signals. Case A: Condition 1:  $x(t) = I \sin(2\pi 56t)$ ,  $y(t) = I \sin(2\pi 56t + \pi/2)$ . Condition 2:  $x(t) = 2 \sin(2\pi 56t)$ ,  $y(t) = I \sin(2\pi 56t + \pi/2)$ . Case B. Condition 1:  $x(t) = I \sin(2\pi 56t)$ ,  $y(t) = 2 \sin(2\pi 56t + \pi/2)$ , Condition 2:  $x(t) = I \sin(2\pi 56t)$ ,  $y(t) = 2 \sin(2\pi 56t + \pi/4)$ .

The application of holospectrum method for practical machine condition monitoring consists in identifying the main frequencies of the rotor vibration signals and constructing the ellipses associated to each frequency of interest. It is expected that any modification in the shaft vibrations produces some modification in the shape of the ellipses (dimensions and inclination angles). The relevant characteristic of the holospectrum method for rotor condition monitoring is that, one can observe the amplitude and phase values of shaft vibration signals in a unique and geometrically simple figure, considering only frequencies that are relevant for fault diagnosis. In this form, the temporal correlation of the signals is preserved in some sense in the holospectrum.

The main difficulty in constructing the holospectrum is that, both amplitude and phase of shaft vibrations must be precisely extracted from the spectral representation. According to the Nyquist theorem, the sampling rate and the period of signal acquisition define the limits of the FFT spectrum resolution, resulting in a limited accuracy in the precise determination of the relevant frequencies. The aliasing errors also could be present in the FFT, even if, a windowing technique has been used in the raw time series. The minimization of errors in the frequency characterization can be achieved by using a high sampling frequency, but this strategy increases the computation time. Other approach is to use an interpolation technique in discrete domain, as has been proposed by Grandke (1983).

In this paper, a high accuracy frequency estimation method, named high resolution spectrum, is proposed for precisely calculation of the spectral parameters, which will be further used for calculation of the holospectrum..

### 3. High-resolution spectrum

The Fourier transform of a continuous signal is mathematically defined for infinite time length signals; however, practical signals measurements limit the signal observation in a period  $T$  of time. Hence, it is necessary to define the continuous fast Fourier transform of a truncated signal  $x(t)$ ,  $0 \leq t \leq T$ , as follows,

$$X(f) = \frac{1}{T} \int_0^T x(t) e^{-j2\pi ft} dt \quad (7)$$

The Eq.(7) must be manipulated into discrete form, so that the sampled values of the signal  $x(t)$  can be used directly in the Eq.(7). To achieve this purpose, one can define the sample interval  $\Delta t = dt$ , the total time  $T = N\Delta t$ , and the elapsed time  $t = k\Delta t$ ,  $k = 0, 1, \dots, N-1$ . The substitution of these parameters into Eq.(7), gives:

$$X(f) = \frac{1}{N\Delta t} \sum_{k=0}^{N-1} [x(k) e^{-j2\pi k\Delta t f}] \Delta t = \frac{1}{N} \sum_{k=0}^{N-1} x(k) e^{-j2\pi k f / f_a} \quad (8)$$

where  $f_a = 1/\Delta t$  is the sampling frequency and the integral has been replaced by a summation over the range  $k = 0$  to  $k = N-1$ .

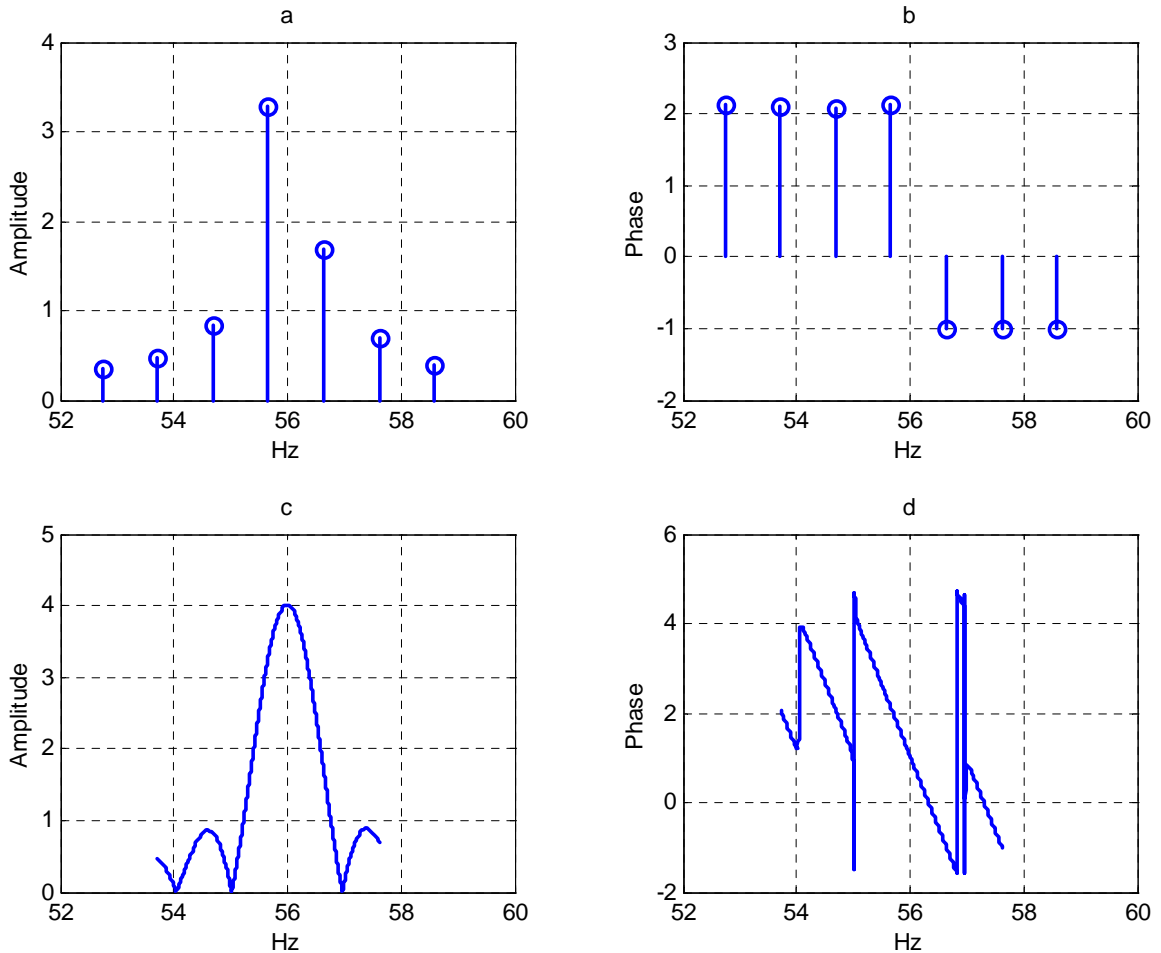


Figure 2. (a) and (b) : Amplitude and phase spectra of  $x(t) = 4\sin(2\pi 56t + \pi/3) + r(t)$  using the FFT Matlab® algorithm for  $f_a = 1\text{ k Hz}$  and  $N = 1024$ . Figure (c) and (d) amplitude and phase spectra using high resolution method.

The Eq.(8) is the continuous Fourier transform version of a discrete signal  $x(k)$  and can now be evaluated for any desired frequency value of interest ( $f_i$ ). The conventional FFT algorithm of the Matlab® software can be used for an

initial estimation of the main frequency of interest with resolution  $\Delta f = N / f_a$ . Once the frequencies of interest of the signal are found, one can evaluate  $X(f)$  over the range  $[f_i - k\Delta f, f_i + k\Delta f]$  for any desired frequency resolution  $\Delta f < N / f_a$ . If only a unique amplitude peak exist in this interval and if  $\Delta f$  is small enough, the frequency correlated with the main lobe can be precisely calculated.

The signal  $x(t) = 4\sin(2\pi 56t + \pi/3) + r(t)$ , where  $r(t)$  is a low intensity random noise, has been used to evaluate the numerical efficiency of the above method. The discrete version of this signal,  $x(k), k = 0, 1, \dots, 1023$ , was defined by using a sampling frequency equal to  $f_a = 1$  kHz and by adopting the noise-to-signal intensity equal to 22% (RMS values). The main frequency of the signal is obviously  $f_i = 56$  Hz, the absolute amplitude is 4 and the phase is  $\pi/3$  rd. The Fig.(2a) and Fig.(2b) show respectively, the absolute amplitude and phase of the spectrum, where the frequency resolution, calculated by FFT Matlab® algorithm is 0.977 Hz and the peak value is estimated at 55.664 Hz. As a result, the amplitude and the phase are not accurately estimated.

To improve the spectrum resolution, a desired frequency resolution  $\Delta f = 0.001$  Hz and a frequency range of [52 - 60] Hz has been defined and used in Eq.(8). The result is an estimated frequency equals to 55.999 Hz. Once the main frequency is calculated, the values of the absolute amplitude and the phase spectra can be easily calculated, resulting in 4.006 and 1.044 rd, respectively. These results are pictured in the Fig.(2c) and the Fig.(2d). The proposed method has been used also for higher noise intensity and the results where very satisfactory. The numerical values of frequency, amplitude and phase, estimated with high resolution could now be used for constructing the ellipses of the holospectrum method.

#### 4. Experimental Results

The holospectrum method has been applied to a vertical test machine for condition monitoring purpose. The vertical test machine is equipped with a vertical rotor coupled to the electric motor by a flexible coupling, which is located at the upper part of the structure. The rotor is supported by rolling bearings and by a hydrodynamic tilting-pad thrust bearing. The axial load applied to the hydrodynamic bearing is provided by a hydraulic mechanism and a load cell measures the applied load intensity. A rigid disc is attached to the lower part of the rotor, where two non-contact inductive probes (Bentley Nevada Proximator® probes), mounted in two orthogonal planes, provide the lateral displacement measurements of the shaft vibrations.

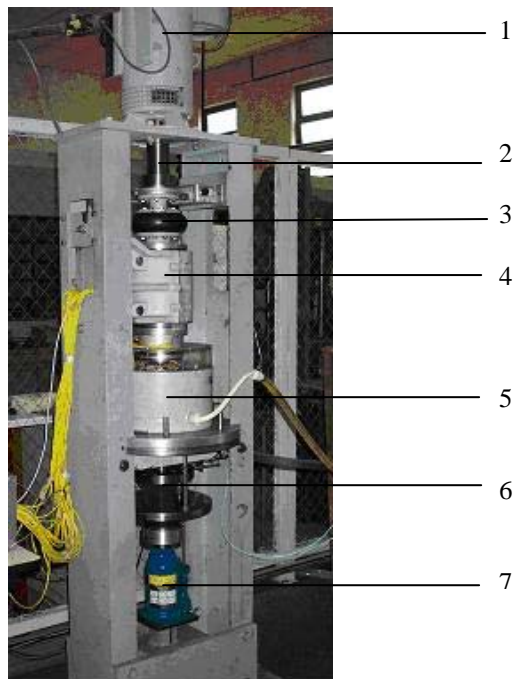


Figure 3. The vertical test machine. 1- Electric motor, 2- rotor shaft, 3- flexible coupling, 4- ball bearing case, 5- hydrodynamic thrust bearing, 6- rigid disc with two non-contact eddy current probes, 6- hydraulic mechanism.

The Lynx® signal analyzer was used for signal acquisition and recording, and the Matlab® software package has been used for all computational calculation of the FFT, the orbit diagram and the holospectrum. The rotor angular velocity was set at 2400 rpm and a sampling frequency of 1 kHz was used for acquisition of the discrete values of  $x(k)$  and  $y(k)$ . Figure (3) shows the vertical machine and its most important components. An automatic oil pump provides

the oil flow rate used for hydrodynamic lubrication. The best oil flow rate for this particular hydrodynamic (Kingsbury KV-9) bearing is about 5 L/s up to 6 L/min. By using a smaller or a bigger value than this, it is expected a small decrease of bearing performance. Insufficient lubrication may cause rotor-stator rubbing, however, if the lubrication is excessive, the rotor may become unstable. In this work, the oil flow rate has been changed from its optimum value and the rotor dynamic behavior has been monitored by the conventional methods and by the holospectrum method. The main objective of this investigation is to verify if variations of these parameters can be detected by the holospectrum method.

The influence of small variations of oil flow rate on the rotor vibrations is now analyzed by using the conventional methods for condition monitoring. The orbit diagrams and the FFT spectrum has been calculated for two different oil flow rates using a sampling period equal to 10 seconds. The Fig.(4) shows that the absolute values of  $X(f)$  and  $Y(f)$  have a small decrease for the synchronous frequency but the second frequency shows negligible amplitude variation. The orbit diagrams pictured in Fig.(5) was calculated using a sampling period equal to 10 s without any average process. It can be seen that the shaft trajectory are virtually the same in these two different machine conditions. The amplitude increase in the synchronous frequency could be interpreted as an increase in the rotor imbalance, but obviously, it is not the case. Thus, it is difficult to diagnose what has been changed in the machine if we look exclusively at the orbit diagrams and spectral representation.

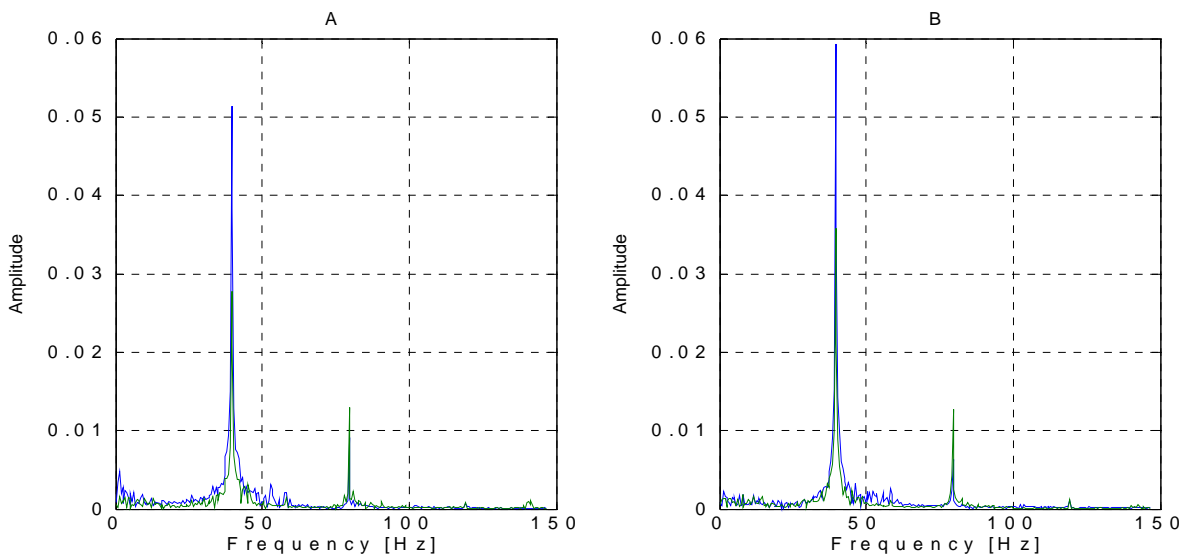


Figure 4 – Absolute amplitudes of radial vibration signals  $X(f)$  and  $Y(f)$ . Case A: Flow rate 6 L/min. Case B: Flow rate 8 L/min.

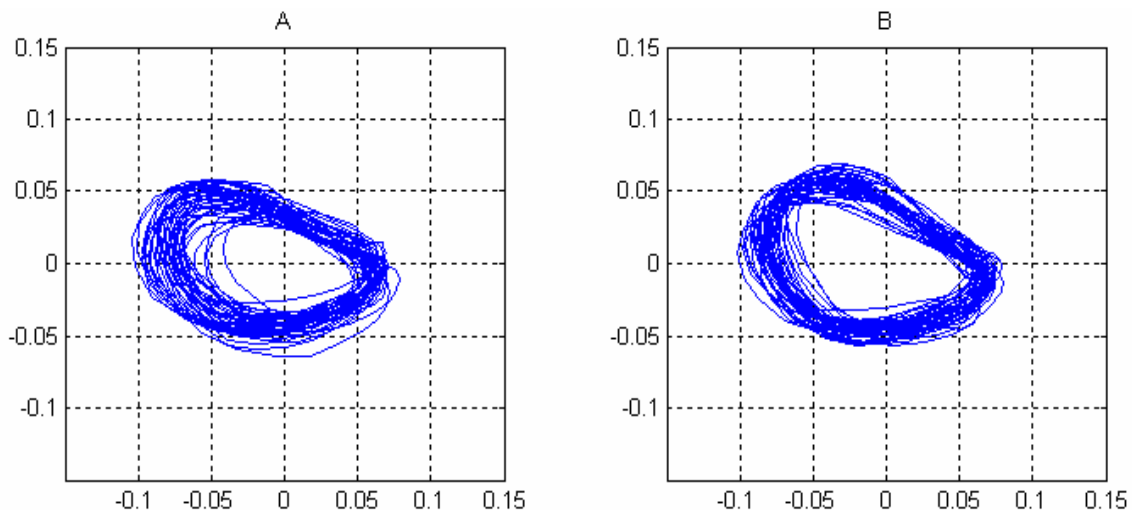


Figure 5. Orbit diagrams pictured for a time length equal to 10 s. Case A: Flow rate 6 L/min. Case B: 8 L/min.

The holospectrum has been calculated for the same above conditions and the results are pictured in Fig. (6). The frequencies of interest, calculated using the high-resolution method are:  $f_1 = 40$  Hz and  $f_2 = 80$  Hz. These frequencies correspond to the rotor angular speed and its second harmonic. The ellipses pictured in Fig. (6A) have different sizes but almost the same phase. This clearly indicates an amplitude increase of the synchronous frequency

when the oil flow rate increases from 6 L/min to 8 L/min. This is an expected result, since a performance deterioration of hydrodynamic bearing occurs for large values of oil flow rate and this fact increases the amplitude of the lateral shaft vibrations at synchronous frequency. The ellipses in Fig. (6B) have clearly different shapes and phases, which indicate a modification in the rotor vibration for the second frequency of interest.

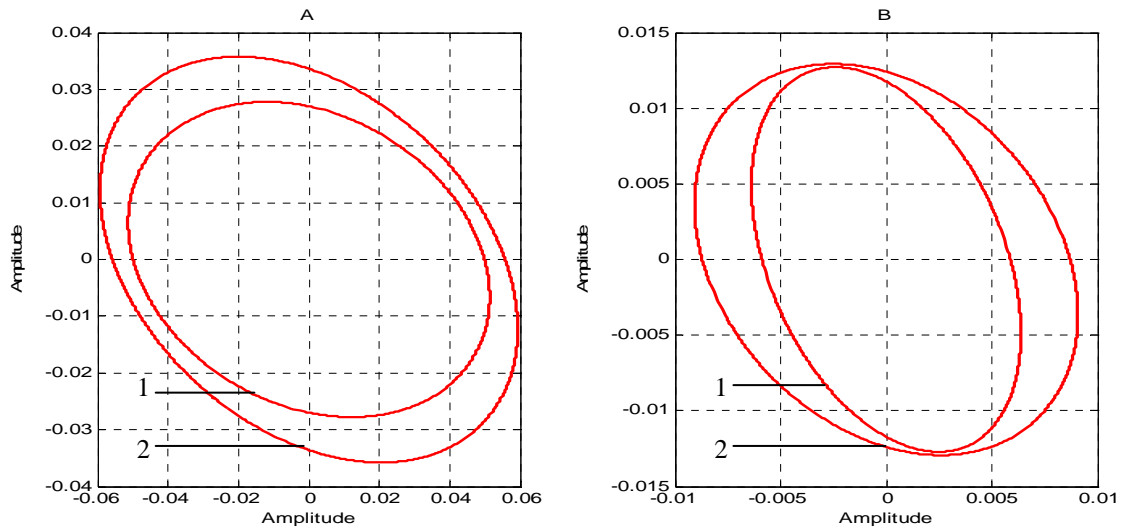


Figure 6. Holospectrum computed for two frequencies of interest. Case A:  $f_1 = 40$  Hz, Case B:  $f_2 = 80$  Hz. Condition 1: Flow rate = 6 L/min. Condition 2: Flow rate 8 L/min.

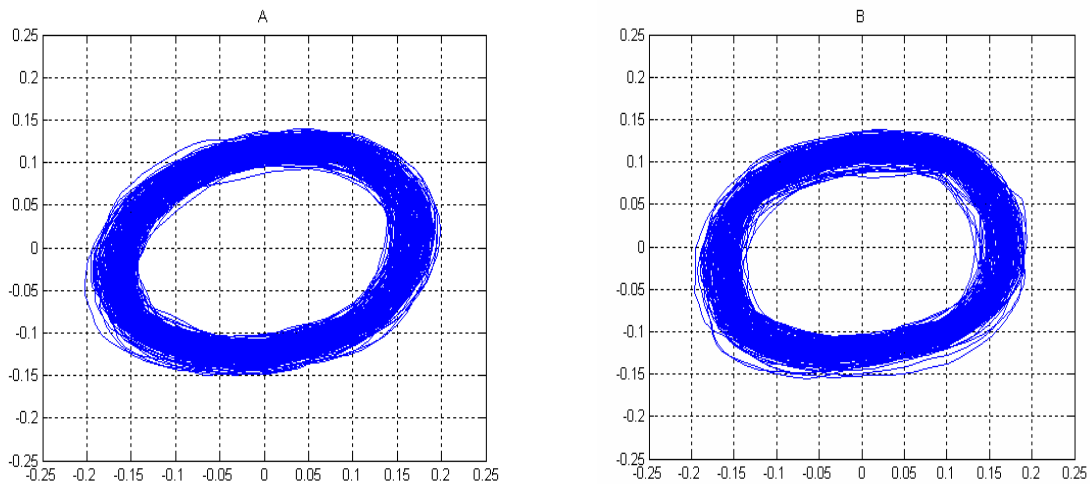


Figure 7. Orbit diagrams pictured for a time length equal to 20 s. Condition A: Axial load = 15 kN. Condition B: Axial load = 20 kN.

It is well known that hydrodynamic thrust bearing introduces more damping in system and also it increases the rotor stability (Jiang, 1999). The axial load applied to the hydrodynamic thrust bearing has been modified from 15 kN up to 20 kN, for investigating its influence on the rotor vibrations. These two different bearing loads have been monitored by the orbits diagrams and by the holospectrum method. The oil flow rate was set at 5 liters per minute and the rotation is 1000 rpm. The orbit diagrams pictured in Fig.(7) shows, for both conditions, a stable, smooth and very similar trajectory pattern, which rise difficulties in observing any system modifications. The respective holospectrum calculated for the synchronous frequency are virtually the same for two different bearing loads, as shown in Fig.(8A). In this case, the system damping increase is not large enough to produce any modification in the holospectrum calculated for the synchronous frequency. However, the holospectrum calculated for the second frequency, pictured in Fig.(8B), shows clearly an amplitude decrease and also a phase modification, which clearly indicates an attenuation of the rotor oscillation for the second frequency. Hence, this holospectrum shows that the rotor trajectory is not exactly the same for slightly different axial bearing loads.

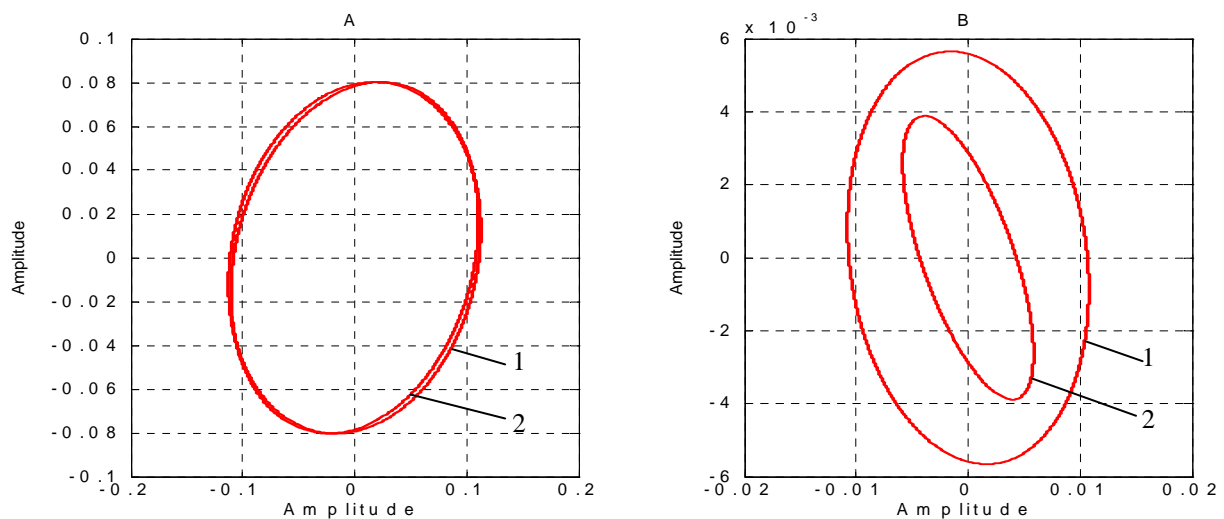


Figure 8. Holospectrum computed for two frequencies of interest. Case A:  $f_1 = 40$  Hz, Case B:  $f_2 = 80$  Hz. Condition 1: Axial load = 15 kN. Condition 2: Axial load = 20 kN.

## 5. Conclusion

A rotating test machine has been used for practical evaluation of three condition monitoring methods. The spectral analysis and orbit diagrams have been compared with the holospectrum method for detecting small variations in the oil flow rate used for hydrodynamic lubrication. The spectral lines and the orbit diagrams showed virtually the same pattern for two different oil flow rates, however, the differentiation of these two conditions are clearly detected in the holospectrum method. The same analysis was applied to different axial loads and the results showed that the detection of small dynamic modification is clearly visible in the holospectrum by comparing the ellipses calculated for different frequencies of interest. The ellipses in the holospectrum are geometrically well defined by mathematical equations and this feature facilitates the task of detecting any small modification in its size; shape and inclination angle, once the influences of other frequencies and noise are both eliminated. The holospectrum is calculated with previously defined frequencies of interest hence, the amplitude and phase values of each relevant frequency must be precisely calculated; otherwise, large errors can be introduced in the holospectrum. The high resolution method proposed for calculating the frequencies of interest, phase and amplitude is mathematically simple and showed satisfactory results within a desired frequency resolution.

## 6. Acknowledgements

The financial support, provided by CNPq and FAPEMIG, is greatly appreciated.

## 7. References

- Cempel, C., 2003, "Multidimensional Condition Monitoring of Mechanical Systems in Operation". *Mechanical Systems and Signal Processing*, 17(6), pp.1291-1303.
- Chen, Y. D., Du, R., Qu, S. L., 1995, "Fault features of Large Rotating Machinery and Diagnosis Using Sensor Fusion". *Journal of Sound and Vibration*, 188(2), pp.227-242.
- Chiarello, A. G., Schwarz, V. A., 2003, "Radial Vibration Analysis of a Vertical Rotor With a Tilting Pad Thrust Bearing". *Proceeding of 17<sup>th</sup> International Congress of Mechanical Engineering*, São Paulo, Brazil.
- Grandke, T., 1983, "Interpolation Algorithm for Discrete Fourier Transforms of Weighed Signals". *IEEE Transactions IM* 32, pp 350-355.
- Jiang, P. L., Yu, L., 1999, "Effect of a Hydrodynamic Thrust Bearing on the Statics and Dynamics of a Rotor-Bearing System", *Mechanics Research Communications*, Vol.25, 2, pp. 219-224.
- Peng Z., He, Y., Chen, Z., Chu, F., 2002, "Identification of The Shaft Orbit for Rotating Machines Using Wavelet Modulus Maxima". *Mechanical Systems and Signal Processing*, 16(4), pp. 623-635.
- Qu, L., Y. Chen, X. L., 1989, "A New Approach to Computer Aided Vibration Surveillance of Rotating Machinery", *International Journal of Computer Applications in Technology*, 2, pp.108-117.
- Qu, L., Liu, X., Peyonne, G., Chen, Y., 1989, "The Holospectrum: a New Method for Rotor Surveillance and Diagnosis", *Mechanical System and Signal Processing* 3, 255-267.
- Shi, D. F., Wang, W. J., Unsworth, P. J., Qu, L. S., 2004, "Purification and Feature Extraction of Shaft Orbits For Diagnosing Large Rotating Machinery". *Journal of Sound and Vibration – Article In Press*.